Atmos. Chem. Phys., 10, 5551–5563, 2010
www.atmos-chem-phys.net/10/5551/2010/
doi:10.5194/acp-10-5551-2010

Atmospheric Chemistry and Physics

Chemical evolution of secondary organic aerosol from OH-initiated heterogeneous oxidation

I. J. George[1,*] **and J. P. D. Abbatt**[1]

[1]80 St. George Street, Department of Chemistry, University of Toronto, Toronto, Ontario M5S 3H6, Canada
[*]now at: School of Chemistry, University of Leeds, Leeds, LS2 9JT, UK

Received: 22 January 2010 – Published in Atmos. Chem. Phys. Discuss.: 5 February 2010
Revised: 4 June 2010 – Accepted: 8 June 2010 – Published: 22 June 2010

Abstract. The heterogeneous oxidation of laboratory Secondary Organic Aerosol (SOA) particles by OH radicals was investigated. SOA particles, produced by reaction of α-pinene and O_3, were exposed to OH radicals in a flow tube, and particle chemical composition, size, and hygroscopicity were measured to assess modifications due to oxidative aging. Aerosol Mass Spectrometer (AMS) mass spectra indicated that the degree of oxidation of 200 nm diameter SOA particles was significantly enhanced due to OH-initiated oxidation, as evidenced by the increase in the fraction of *m/z* 44 fragment of total organic mass concentration (F44). F44 values of the SOA particles, initially in the range F44=0.04–0.07, increased by up to ΔF44$\sim$0.01 under equivalent atmospheric aging timescales of 2 weeks, assuming a 24-h average OH concentration of 10^6 cm^{-3}. Particle O/C ratios calculated from F44 values, initially in the range O/C=0.25–0.35, rose by a maximum of ΔO/C$\sim$0.04 units for 2 weeks of aging. Particle densities also increased with heterogeneous oxidation, consistent with the observed increase in the degree of oxidation. Minor reductions in particle size, with volume losses of up to 10%, were observed due to volatilization of oxidation products. The SOA particles activated more readily to form cloud droplets with an increase in the κ hygroscopicity parameter of up to a factor of two for the equivalent of 2 weeks of OH atmospheric exposure. These results indicate that OH heterogeneous oxidation of typical SOA needs to be considered as an atmospheric organic aerosol aging mechanism, most likely of higher relative importance away from VOC source regions, where other aging mechanisms are less dominant.

Correspondence to: I. J. George
(igeorge@leeds.ac.uk)

1 Introduction

Atmospheric aerosol particles play an important role in climate, visibility, atmospheric chemistry and human health. Condensed-phase organic matter represents a significant mass fraction (20–90%) of submicron atmospheric aerosol (Kanakidou et al., 2005). Primary organic aerosol (POA) particles are directly emitted into the atmosphere through combustion, biomass burning and vegetation. Secondary organic aerosol (SOA) mass is produced by the gas-phase oxidation of biogenic and anthropogenic volatile organic compounds (VOCs) to form more oxygenated, lower volatility species that readily partition into the particle phase. The impact of atmospheric organic aerosols on climate and other environmental processes is ultimately contingent upon their physico-chemical properties, such as chemical composition, size, density and hygroscopicity. Given the high degree of chemical complexity of organic matter in atmospheric aerosols, there has been a large effort over the last decade to characterize the chemical nature and particle properties of atmospheric aerosols (Goldstein and Galbally, 2007; Robinson et al., 2007; Heald et al., 2008; Jimenez et al., 2009) and their direct and indirect effects on climate (Kanakidou et al., 2005).

The chemical and physical properties of organic aerosols (OA) can be modified in the atmosphere by several processes, collectively referred to as chemical aging, which often result in the conversion of the chemical nature of particulate organic matter from hydrophobic to hydrophilic. Atmospheric chemical aging of OA includes coagulation with aged particles, condensation of soluble inorganic species and oxidized organic gases to form SOA, condensed-phase reactions within the particle leading to oligomer formation, cloud processing and multi-phase reactions, and heterogeneous oxidation of OA by gas-phase oxidants (e.g. OH, O_3, NO_3, Cl). Heterogeneous oxidation has received attention

recently because it is poorly understood (Rudich et al., 2007). Laboratory investigations of atmospheric OA oxidation processes have mainly involved the heterogeneous oxidation of single-component hydrophobic particles as models for POA, e.g. the reaction of O_3 with oleic acid particles (Zahardis and Petrucci, 2007). A number of recent studies have investigated the heterogeneous oxidation of laboratory particles and films containing saturated organic matter by atmospheric gas-phase radicals, such as OH, NO_3 and Cl (Bertram et al., 2001; Moise and Rudich, 2001; Eliason et al., 2004; Molina et al., 2004; Knopf et al., 2006; Lambe et al., 2007; George et al., 2007; Hearn et al., 2007; McNeill et al., 2008; Vlasenko et al., 2008; Gross and Bertram, 2009; Gross et al., 2009; Renbaum and Smith, 2009; Smith et al., 2009). These studies have shown that the heterogeneous kinetics for the uptake of OH onto model POA are rapid and efficient. Furthermore, chemical aging by OH radicals leads to more oxygenated condensed-phase organic species and volatilization of gas-phase products with an observed reduction in particle size to variable degrees depending on composition of the organic matter and its phase. Chemical aging has recently been shown to enhance hygroscopicity of OA, e.g. increasing the cloud condensation nucleus (CCN) activity of model POA particles that are initially CCN inactive for particle sizes $<$200 nm at supersaturations $<$1% (Broekhuizen et al., 2004; Petters et al., 2006; Shilling et al., 2007; George et al., 2009). We do note though that Petters et al. (2006) have concluded that such mechanisms of increasing aerosol hygroscopicity are likely to be less important than other aging processes, such as condensation of soluble inorganics.

In their analysis of measurements of atmospheric aerosol composition with the Aerosol Mass Spectrometer (AMS) from 37 field studies, Zhang et al. (2007) concluded that oxygenated organic aerosol (OOA) comprises a significant and often dominant fraction of the non-refractory organic aerosol mass in urban and remote regions. The hydrocarbon-like organic aerosol (HOA) fraction that is thought to be closely related to POA was a less important fraction in OA than OOA, especially away from urban regions. Several field studies have measured a concomitant increase in organic mass and degree of oxidation of OA with photochemical age (de Gouw et al., 2005; McFiggans et al., 2005; Takegawa et al., 2006; Kleinman et al., 2007; Weber et al., 2007), thus suggesting a possible link between the OOA fraction in atmospheric aerosols with SOA formation (Zhang et al., 2005a). Given that almost all laboratory studies on the heterogeneous oxidation of OA used model POA until very recently (George et al., 2008; Jimenez et al., 2009), the relative importance of heterogeneous oxidation as a chemical aging process for more oxygenated OA, such as SOA, under atmospherically relevant timescales remains unclear. Although chamber SOA aging studies show enhancement in oxidation of SOA particles with time (Baltensperger et al., 2005; Alfarra et al., 2006; Sage et al., 2008) particle aging from the gas-phase oxidation reactions and heterogeneous particle oxidation reactions cannot be easily decoupled in these chamber experiments. There is a growing consensus that SOA formation dominates over the aging process leading to an enhanced oxidation state of OA over timescales of several hours given that heterogeneous oxidation is too slow to impact aerosol chemistry on these timescales (Jimenez et al., 2009). Yet, the lifetime of atmospheric aerosols is much longer, typically over a timescale of several days, during which time further aging from heterogeneous oxidation could occur.

The major objective in this study was to assess the importance of heterogeneous oxidation as an aging mechanism for atmospheric aerosols containing oxygenated organic matter. To that end, we investigated the heterogeneous reaction of laboratory SOA used as a model for oxygenated ambient organic aerosols with OH radicals in a reactor flow tube setup. Laboratory SOA was produced from ozonolysis of α-pinene with continuously flowing precursor gases added at relatively high concentrations to produce the high aerosol concentrations required for this work. Even SOA particles produced under controlled laboratory conditions are composed of a highly complex chemical mixture of organic species, making the characterization of molecular level chemical modifications due to aging a non-trivial task. Thus, we focus here on characterizing the modifications of bulk particle chemistry due to oxidative aging using several online particle analysis techniques, including an Aerodyne AMS to measure the overall degree of oxidation and a Thermal Gradient Diffusion Chamber (TGDC) to measure CCN activity. Particle size change measurements monitored by the tandem differential mobility analyzer (TDMA) technique were essential to gauge whether the OH-initiated oxidation pathway leading to fragmentation and potential volatilization of reaction products was an important mechanism. Recent work by Kroll et al. (2009) has suggested the fragmentation mechanism becomes the dominant oxidation mechanism for aerosols containing highly oxygenated organics produced from OH oxidation of model POA. The other reaction pathways lead to the addition of oxygenated functional groups to the organic compounds in the particle phase, thereby increasing the aerosol mass and degree of oxidation of the particle-phase organic material (Molina et al., 2004) We note that although similar in nature to SOA oxidation experiments briefly presented in Jimenez et al. (2009), our study examines the full effects of oxidative processing on the particle degree of oxidation, density, size, and hygroscopicity.

2 Experimental

2.1 Aerosol generation

Secondary organic aerosol particles were produced by the dark reaction of α-pinene (AP) with O_3 in a continuous flow reactor. The O_3 and AP flows were mixed in approximately equal flow rates with a combined flow of 0.3 lpm in a 3 L

Table 1. SOA precursor mixing ratios and particle properties. F44 values are percentages of the fragment *m/z* 44 of total organic mass concentrations in the AMS mass spectrum. Values in brackets are one standard deviation of mean values. O/C ratios were calculated from F44 values (Aiken et al., 2008).

SOA type	$[O_3]$ ppm	[AP] ppm	N $\times 10^3 cm^{-3}$	Org Mass $\mu g\ m^{-3}$	ρ $g\ cm^{-3}$	F44 (%)	O/C
1	75 (9)	6.8 (0.7)	24 (3)	43 (4)	1.23 (0.01)	6.3 (0.3)	0.32 (0.02)
2	10 (1)	5.3 (0.2)	24 (3)	37 (3)	1.246 (0.002)	4.6 (0.5)	0.26 (0.04)
3	11 (1)	0.43 (0.04)	2.9 (0.4)	1.9 (0.3)	1.26 (0.01)	6.9 (0.2)	0.34 (0.01)

glass round bottom flask under dark conditions. The SOA precursor gases were added in a continuous flow under dry conditions at room temperature. The gas flow of AP vapor was produced by passing 5 to 30 sccm of N_2 (BOC, 99.998%) through a fritted glass bubbler containing α-pinene liquid (Fluka, 99.0%) held at temperatures from 263 K to 273 K then further diluted with a N_2 flow. AP mixing ratios ranged from 0.4 to 7 ppm after dilution assuming the AP flow through the bubbler was saturated. Ozone was generated by passing a mixture of N_2 and O_2 (BOC, 99.6%) over a 22.9-cm long mercury penray lamp (UVP). O_3 concentrations were measured prior to mixing with the AP flow in a 14-cm long UV absorption cell at a wavelength of λ=254 nm, where O_3 mixing ratios ranged between 9 to 83 ppm. To study whether SOA precursor concentrations affect SOA composition and OH oxidation, AP and O_3 were varied to either relatively high or low concentrations, i.e. the extreme values of the achievable experimental range of precursor concentrations in this work. SOA particles were produced under three sets of conditions by varying the SOA precursor gas mixing ratios: a) SOA1 particles produced under high AP (6.8 ppm), high O_3 (75 ppm), b) SOA2 particles produced under high AP (5.3 ppm), low O_3 (10 ppm), c) SOA3 particles produced under low AP (0.43 ppm), low O_3 (11 ppm). Table 1 summarizes the precursor mixing ratios and particle properties for 200 nm diameter SOA particles for all three SOA types. Before introduction into the reactor flow tube setup, the SOA flow from the SOA generation flask was passed through an O_3 removal denuder (Carus, Carulite 200) and two activated carbon denuders (Sigma-Aldrich, 4–14 mesh) to remove unreacted precursor gases and volatile products.

2.2 SOA Oxidation Experiment

Monodisperse 200 nm SOA particles were exposed to OH radicals in the absence of NO_x in a reactor flow tube setup, which has been described in greater detail previously (George et al., 2007) and will be described here briefly. The polydisperse SOA flow (0.3 lpm) was passed through an aerosol neutralizer (TSI 3077), then particles were size selected with a Differential Mobility Analyzer (TSI 3081) at a mobility diameter of 200 nm. Monodisperse SOA particles were entrained in the combined humidified/O_3 flows (when O_3 was present) in a balance of N_2 and O_2 gases and passed into a Pyrex mixing volume (0.8 L) with a residence time of approximately 80 to 110 s, then into the reactor flow tube where particles were exposed to OH radicals. The flows containing water vapour and ozone were added as precursor gases for photochemical OH production as described below. Experiments were conducted under atmospheric pressure (1 atm), room temperature (24 °C) and in the relative humidity range of 19 to 50%.

OH radicals (10^9 to $10^{10}\ cm^{-3}$) were produced in the reactor flow tube by passing O_3 over a 22.9 cm long, O_3-free Hg Pen-ray lamp (UVP) in the presence of water vapor. The reactor flow tube Hg lamp housing was pre-treated to filter out O_3-forming 185 nm light. Particle oxidation experiments were performed at room temperature. O_3 was produced as an OH precursor for the particle oxidation experiment by passing a dry flow of mixed O_2 and N_2 through an O_3 generator (Jelight model 1000). An O_2 flow (0.12 lpm) was also added to this O_3 flow for most experiments to maintain the experimental O_2 mixing ratios ($\sim 2\times 10^5$ ppmL) to near atmospheric levels. No clear distinction in the data due to variable O_2 mixing ratios was observed. O_3 mixing ratios were 0.11–54 ppm after dilution with other flows. The relative humidity in the reactor flow tube ranged from 19 to 50%, which was measured by a hygrometer (VWR, $\pm$1%). In a separate set of experiments, the steady-state OH radical concentrations were measured by reaction with SO_2 (Matheson, 99.98%). The SO_2 loss from its reaction with OH was monitored with a chemical ionization mass spectrometer in negative-ion mode using SF_6^- as the reagent ion. We used a photochemical model to calculate steady-state OH concentrations based on experimental O_3 concentrations and RH values (George et al., 2007). We report an uncertainty in the OH concentrations of 50% based on accuracy of the photochemical model to predict measured OH concentrations under a range of conditions and the variation in OH measurements with time.

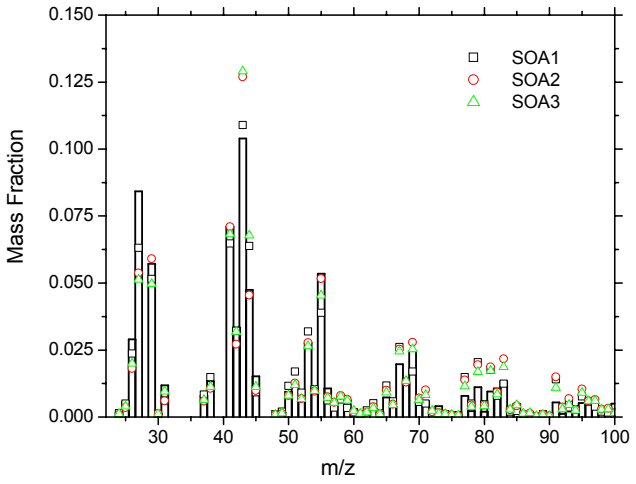

Fig. 1. Mass spectra of SOA1, SOA2, SOA3 in symbols and chamber SOA in bars (Bahreini et al., 2005) Mass spectra are normalized to unity.

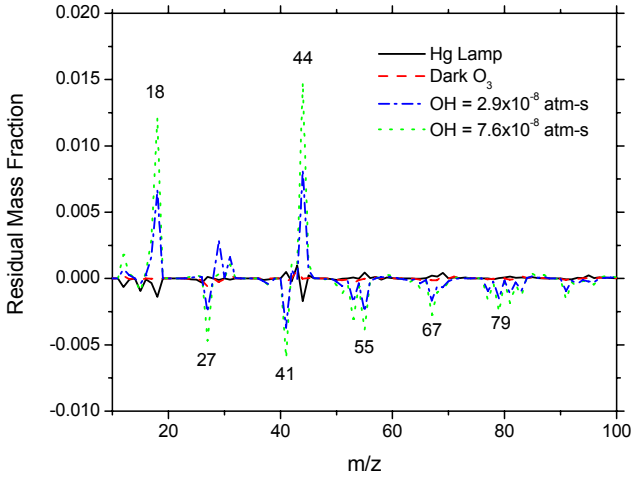

Fig. 2. Difference organic mass spectra of SOA1 for control conditions Hg Lamp and Dark O_3 subtracted from Dark mass spectra. Mass spectra for SOA exposed to OH were subtracted from Hg Lamp mass spectra. OH exposures are indicated. SOA1 is shown only as an example; similar behavior was observed for SOA2 and SOA3.

2.3 Particle characterization

The evolution in monodisperse SOA particle composition and properties from OH-initiated oxidation was measured using a suite of particle analysis techniques, which sampled the aerosol flow after particles passed through the reactor flow tube and a second O_3 denuder. Size distributions of monodisperse SOA were measured with a Scanning Mobility Particle Sizer (SMPS, TSI 3080) with a condensation particle counter (CPC, TSI Model 3010). The size-resolved chemical composition of monodisperse SOA was measured using a time-of-flight aerosol mass spectrometer (c-ToF-AMS; Aerodyne Research, Inc.) (Jayne et al., 2000; Drewnick et al., 2005). The AMS measurements alternated between mass spectrum (MS) and particle time-of-flight (PTOF) modes, where the latter sampling mode gave aerosol composition as a function of particle vacuum aerodynamic diameters. ToF-AMS data were analyzed using the ToF-AMS Analysis Toolkit v.1.43 for use in Igor Pro software (Wavemetrics, Inc.). Filter measurements were taken in order to adjust the air contribution to the mass spectrum, particularly the gas phase CO_2 contribution to *m/z* 44. AMS and SMPS measurements were taken concurrently with AMS averaging and SMPS scanning time of 3 min per sample. AMS organic mass spectra for the three types of SOA particles (i.e. SOA1, SOA2, SOA3) shown in Fig. 1 were similar ($R^2 > 0.9$, for comparison of one spectrum to another), despite the large differences in precursor concentrations (Table 1) and were generally consistent with the α-pinene + O_3 chamber SOA mass spectrum from Bahreini et al. (2005) ($R^2 > 0.9$).

Positive Matrix Factorization (PMF), a factor analysis technique (Paatero and Tapper, 1994; Paatero, 1997; Lanz et al., 2007), was applied to deconvolve AMS organic mass spectra of the SOA particles to further illustrate the changes in chemical composition of the SOA particles resulting from OH oxidation. In PMF analysis, the SOA spectra were deconvolved into organic components with only positive contributions to the dataset by solving the following equation:

$$\mathbf{X} = \mathbf{GF} + \mathbf{E} \quad (1)$$

In this case, the input data matrix **X** has rows of measured average ToF-AMS mass spectra and columns of the time series for each *m/z* sample. Matrix **G** contains columns of the time series mass contribution (in $\mu g\, m^{-3}$) of the deconvolved factor and the rows of matrix **F** are the factor profiles. The residuals that were not fit by the PMF analysis are represented as matrix **E**. The PMF model solves Eq. (1) for matrices **G** and **F** to minimize the residuals using a weighted least-squares algorithm based on the input uncertainty in the data set. We utilized the CU AMS PMF Tool developed by Ulbrich et al. (2009) used in the Igor Pro software to perform the PMF analysis of the AMS data (272 data points) in robust mode, which included organic mass spectra of all organic mass contributions with *m/z* values $\leq$200 (170 *m/z*'s).

For the PMF analysis, we used oxidation data for SOA1 with 2 factors (A1–A2) giving the most reasonable solution. Further information on the PMF analysis including how the number of factors was determined is provided in the Supplementary Material. Because the chemical composition of the SOA particle types varied slightly, a PMF analysis including all three SOA types (i.e. SOA1, SOA2 and SOA3) together required three factors to fully account for initial composition, which complicated interpretation of the results and did not provide more information than the PMF analysis of SOA1 only. Therefore, we focused on the PMF analysis of SOA1 for simplification, but we note that the PMF factors

from analysis of the combined SOA types followed similar trends with oxidation as the 2-factor solution for the SOA1 dataset (i.e. the more oxygenated factors increased by similar percentage with OH exposure relative to I_0 values).

The CCN activity of the SOA particles (SOA1 and SOA2) was measured with a continuous flow thermal gradient diffusion chamber (TGDC), which has been described in detail elsewhere (Kumar et al., 2003). For the CCN experiments, we note that, unlike the previous experiments, polydisperse SOA particles from the SOA generation flask were introduced into the particle oxidation flow tube setup. Particles were then size-selected with a DMA after passing through the oxidation setup. The flow was diluted with a N_2 flow by factor of two, and the number concentrations of monodisperse aerosols, ranging from 0 to $\sim 10^4\,cm^{-3}$, were measured with a CPC. Concurrently, the aerosol flow was sampled with the TGDC exposing particles to supersaturated conditions with respect to water that were controlled by the TGDC wetted plate temperatures. The number concentrations of activated droplets (D>0.5 µm) were measured with an aerodynamic particle sizer (TSI 3320). TGDC saturations were calibrated using ammonium sulfate particles produced by an atomizer (TSI 3076). Experimental activation diameters (D_{act}), defined as the inflection point on the sigmoidal fit of a plot of CCN/CN versus particle dry diameter, were translated to effective supersaturation S_{eff} values using a hygroscopicity parameter value of κ=0.61 (Petters and Kreidenweis, 2007; George et al., 2009).

3 Results and discussion

3.1 Particle oxidation

The AMS mass spectra of 200 nm SOA particles exposed to OH radicals in the reactor flow tube were compared to control conditions to gauge the effect of OH oxidation on the particle composition, in particular on the overall degree of oxidation. The modification of the organic mass spectra of SOA1 particles due to varying flow tube conditions is displayed in the difference spectra in Fig. 2. The uncertainty in the measurements was determined under control conditions, i.e. reactor flow tube conditions in the absence of OH radicals, including the following conditions: (a) dark conditions with O_3 absent ("Dark"), (b) the Hg lamp in the reactor flow tube turned on with O_3 absent ("Hg Lamp"), and (c) O_3 present with Hg lamp off ("Dark O_3"). The SOA organic mass spectra in Fig. 2 taken under two OH exposures were clearly altered compared to the Hg Lamp and Dark O_3 control conditions. OH exposure led to an increase in *m/z* 18 (H_2O^+) and 44 (CO_2^+) mass fractions, which are typically associated with carboxylic acids, and a reduction in most other major peaks, such as masses that are typically associated with hydrocarbons (e.g. *m/z* 41, 55), indicating that SOA became more oxygenated with increasing OH exposure.

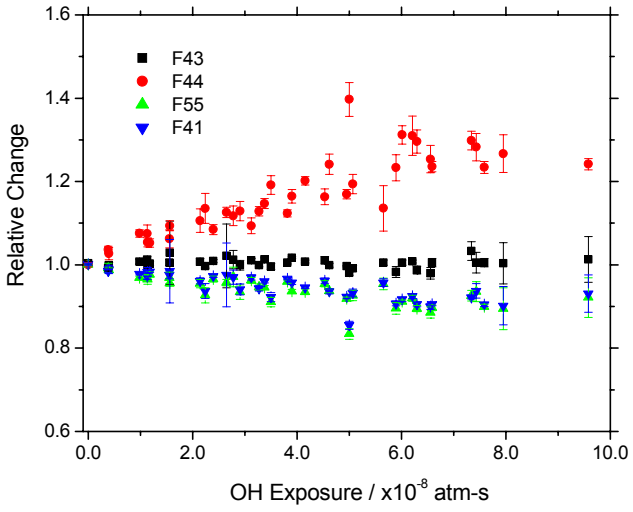

Fig. 3. Relative changes in F41, F43, F44 and F55 with OH exposure for all SOA types, i.e. SOA1, SOA2 and SOA3 data are all plotted together. Error bars represent one standard deviation of average values.

Mass fragments *m/z* 44 and 57 ($C_4H_9^+$) have been used as mass tracers for OOA and HOA fractions, respectively in AMS mass spectra of ambient OA (Zhang et al., 2005b). The mass fractions *m/z* 44 and 55 of total organic, now referred to as F44 and F55, respectively, are used here to observe changes in the degree of oxidation of SOA particles with heterogeneous oxidation. We used *m/z* 55 in place of *m/z* 57 because *m/z* 57 is a minor peak in the SOA spectra and *m/z* 55 can also be an important mass fragment in HOA. For the following analysis, SOA mass spectra for particles exposed to OH radicals (I) were compared to average Hg Lamp mass spectra (I_0) taken before and after the oxidized SOA mass spectra. Relative changes (I/I_0) in F44 and F55 mass fractions of SOA particles were monitored under a range of OH exposures in Fig. 3. Trends for all SOA types (SOA1, SOA2 and SOA3) were consistent and so were not distinguished in the plot.

Figure 3 shows a clear trend of increasing F44 and decreasing F55 with OH exposure up to 8×10^{-8} atm-s. In contrast, the mass fraction of *m/z* 43 that typically contains both hydrocarbon and oxygenated organic fragments ($C_3H_7^+$, $C_2H_3O^+$) showed little change with oxidation. High resolution ToF-AMS measurements of chamber α-pinene SOA particles revealed that *m/z* 55 also represents mass fragments from oxygenated and hydrocarbon components ($C_3H_3O^+$, $C_4H_7^+$) (Shilling et al., 2009). Nevertheless, we found that the mass fraction for *m/z* 55 followed a similar trend with OH exposure as mass *m/z* 41 that is expected to be mostly made up of a hydrocarbon fragment ($C_3H_5^+$) (Shilling et al., 2009). Taking the trend for all SOA types, the F44 and F55 fractions were altered by +21% and −7% from initial values, respectively, for an equivalent atmospheric exposure of

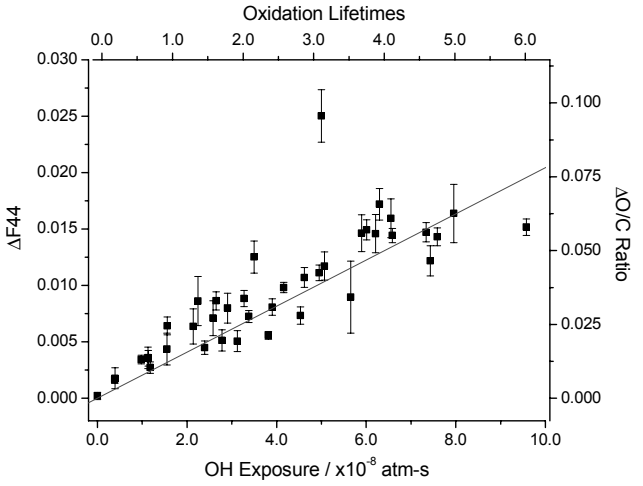

Fig. 4. Change in F44 and the O/C ratio as a function of OH exposure (bottom x-axis) and oxidation lifetime (top x-axis) for all SOA types (SOA1, SOA2, SOA3). O/C ratios were calculated from (Aiken et al., 2008). Error bars represent one standard deviation of ΔF44 values. Line represents error-weighted linear fit to the data forced through origin ($f(x)=(2.04(\pm0.03)\times10^5)x$; $R^2=0.87$).

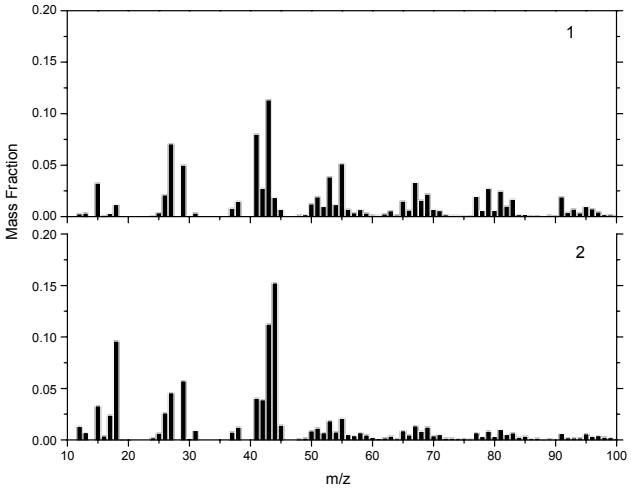

Fig. 5. PMF profiles for A1 and A2 PMF factors deconvolved from SOA1 oxidation data.

2 weeks for a 24-h average OH concentration of 10^6 cm^{-3} corresponding to an experimental OH exposure of approximately 5×10^{-8} atm-s.

These results are comparable to our recent work on OH-initiated heterogeneous oxidation of ambient aerosol (George et al., 2008), where we observed an average relative increase of +23% in F44 values over a similar range of OH exposures for ambient aerosol with initial F44 fractions between F44=0.06–0.13. In contrast, we measured more dramatic changes of approximately a factor of 3 increase in F44 for the oxidation of less oxygenated model primary organic aerosol (POA) particles with an initial F44 fraction of F44=0.011 (George et al., 2007). Therefore, a comparison of this work with our previous OH oxidation studies for model POA and ambient aerosols indicate that heterogeneous oxidation leads to consistent enhancement in F44 mass fraction of ΔF44=0.01–0.02 on an absolute scale for 2 weeks of aging representing a reasonable upper limit of aging time in the atmosphere. Yet, aging may bring about a greater relative enhancement in particle oxidation state for POA compared to oxygenated organic aerosols because of the lower initial oxidation state of POA particles.

We applied the observed correlation between O/C ratios and F44 from AMS measurements of ambient and laboratory OA in recent work by Aiken et al. (2008) to calculate absolute changes in O/C ratios with OH oxidation directly from our observed F44 measurements as shown in Fig. 4. Because we do not have direct measurements of elemental composition of the SOA particles in this work, we make the assumption that the relationship between O/C ratios to F44 from Aiken et al. (2008) holds true for the laboratory SOA in this work as it does for chamber and ambient SOA in that study. Average values for initial O/C ratio values for three types of SOA are stated in Table 1. It was found that the O/C ratios were calculated to be initially in the range of O/C=0.25–0.35, then rose to a maximum of O/C=0.4–0.45 with OH oxidation, Our work suggests that the maximum absolute change in the O/C ratio expected from OH oxidation would be between approximately ΔO/C=0.04–0.08 units for two weeks of equivalent atmospheric OH exposure time. The lower limit is from this work with SOA particles, and the upper value is from our BES particle oxidation (George et al., 2007). Kroll et al. (2009) measured the evolution of the O/C ratios of squalane particles with OH oxidation with a high resolution ToF-AMS. Squalane particles became as oxidized as the initial SOA1 particle composition in this work after approximately 12 "oxidation lifetimes" (i.e. the total OH reactive collisions with a particle normalized to total number of organic molecule in the particle). Further, we found that the O/C ratio increased by ΔO/C∼0.04 in three subsequent oxidation lifetimes that correspond to approximately 2 weeks of aging in this work. Thus, our work is consistent with the observed changes in O/C ratios for OH oxidation of squalane particles (Kroll et al., 2009).

The deconvolved PMF factors from oxidized SOA mass spectra in this work were compared with organic aerosol source factors deconvolved from ambient AMS measurements (i.e. OOA- and HOA-like factors) as a means for evaluating the atmospheric relevance of the observed changes in degree of oxidation of the OA particles. The two PMF factor profiles (A1 and A2) deconvolved from the SOA1 data are shown in Fig. 5. The PMF factors as well as mass spectra for initial and oxidized SOA1 were compared to several HOA-like and OOA-like PMF profiles (Lanz et al., 2007; Ulbrich et al., 2009; Slowik et al., 2009) with R^2 values sum-

Table 2. R^2 values of PMF factors A1 and A2 in this work compared to laboratory chamber SOA (Bahreini et al., 2005) and PMF factors from ambient data for the following studies: Zurich (Lanz et al., 2007), Egbert (Slowik et al., 2009), Pittsburgh (Ulbrich et al., 2009). Oxidized SOA1 mass spectrum was taken under an OH exposure of 7.6×10^{-8} atm-s.

	Initial SOA1	Oxidized SOA1	A1	A2
Chamber SOA	0.95	0.92	0.87	0.65
Zurich OOA1	0.53	0.62	0.11	0.86
Egbert OOA1	0.46	0.55	0.14	0.82
Pittsburgh OOA1	0.71	0.78	0.36	0.91
Zurich OOA2	0.69	0.65	0.76	0.36
Egbert OOA2	0.86	0.92	0.55	0.93
Pittsburgh OOA2	0.62	0.68	0.38	0.71
Zurich HOA	0.33	0.32	0.38	0.16
Egbert HOA	0.75	0.68	0.94	0.33
Pittsburgh HOA	0.69	0.65	0.75	0.39

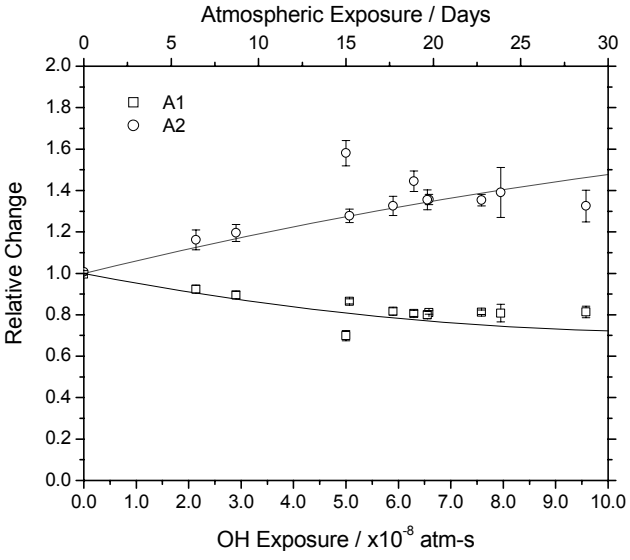

Fig. 6. Relative changes in time series mass contributions of PMF factors A1 and A2 (deconvolved from SOA1 oxidation data) with OH exposure with bottom x-axis in experimental exposure, top x-axis in atmospheric exposure time assuming [OH]=1×10^6 cm^{-3}. Lines are to guide the eye. Error bars represent one standard deviation of average values.

marized in Table 2. Ambient OOA1 is generally more oxygenated than OOA2, and represents low-volatility aged regional OA, whereas OOA2 is more volatile and likely more recently formed. The A1 factor (F44∼0.02) correlated with some of the HOA factors and chamber SOA (Bahreini et al., 2005), suggesting that it may be representative of the less oxygenated component of SOA that reacts away with OH exposure. OOA1 factors correlated well with the A2 factor (F44∼0.15). Note that this comparison analysis does not imply that the SOA PMF factors in this work represent organic mass of similar chemical composition to ambient PMF factors.

The relative changes in the mass fractions of the PMF A1 and A2 factors of the summed PMF factor organic mass concentrations (i.e. these organic mass concentrations were correlated with measured values with slope=1.002 and R^2=0.9999) due to OH exposure are shown in Fig. 6. The HOA-like A1 PMF factor, representing 66(±2)% of SOA1 organic mass before oxidation, decreased significantly with OH exposure similar to the observed reduction in F55 ($R^2 > 0.9$). The OOA1-like factor A2 correlated with increases in F44 ($R^2 > 0.74$) with OH exposure. In this respect, our results are similar to those presented recently by Jimenez et al. (2009), where oxidized mass spectra increasingly resembled low volatility OOA factors. Also, this validates that the specific *m/z* masses 44 and 55 are responding to changes in the overall mass spectrum, and F44 and F55 are good proxys for the PMF factors in this study. For one day of equivalent atmospheric OH exposure, relative changes in the PMF factors were just discernible within uncertainties. After two weeks of OH exposure however, the mass concentration of the OOA-like factor increased from 34% to ∼45% of the organic mass. The comparison of the initial and oxidized SOA1 with the ambient PMF factors suggest that although the particles are becoming more like OOA1, they are not completely converted to OOA1 even at high OH exposures. In particular, the O/C ratio of the SOA changed from the range of 0.25 to 0.35 up to a maximum of 0.45 upon the highest levels of oxidation, distinctly lower than the O/C of ambient OOA1 (i.e. O/C≈0.5–0.9) (Ng et al., 2009).

3.2 Modification of particle properties

Figure 7 shows the relative changes in SMPS particle volume normalized to particle number concentrations for 200 nm diameter SOA particles. Under control conditions including Hg Lamp experiments, the variability in the particle volume measurement was within 5%. Particle volumes decreased with OH exposure to a maximum loss of approximately 10% particle volume at the highest OH exposures. For comparison, we have observed a maximum of 17% decrease in particle volume for Bis(2-ethylhexyl) sebacate (BES) particles (George et al., 2007) and up to 50% loss for stearic acid particles (George et al., 2009). A comparison with the Kroll et al. (2009) work as outlined previously for the changes in O/C ratios reveals that oxidized squalane particles underwent a reduction in particle volume of 9% for 3 OH lifetimes assuming initial O/C ratios of the SOA particles here. Therefore, even though the fragmentation pathway may be the dominant oxidation pathway for OH oxidation of oxygenated OA as determined by Kroll et al. (2009) for oxidized squalane particles, it nevertheless leads to minor reductions in particle volume.

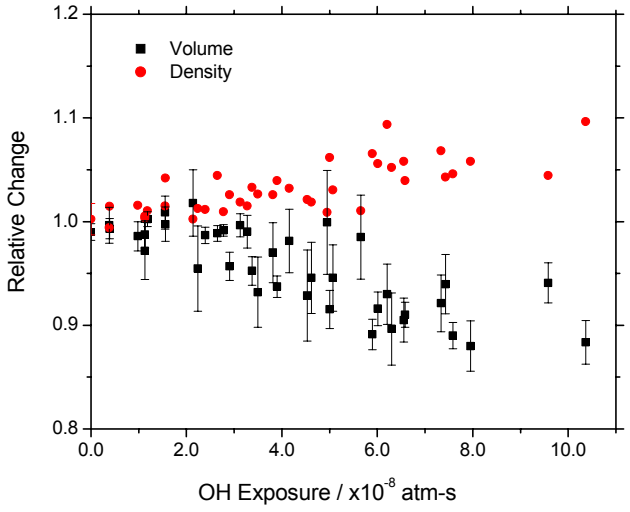

Fig. 7. Relative changes in volume and density with OH exposure for all SOA types.

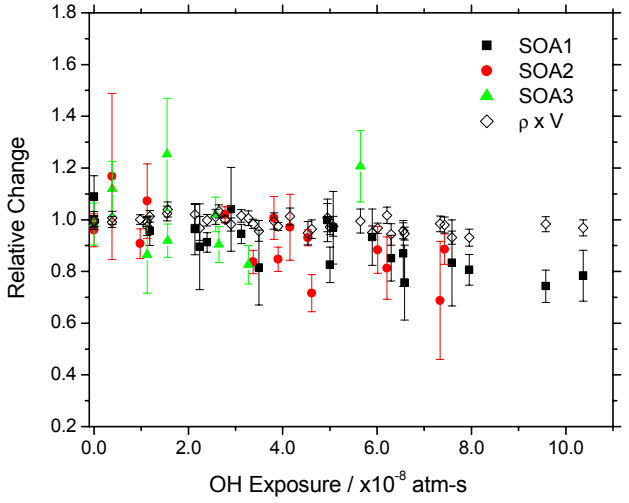

Fig. 8. Relative changes in SOA organic mass. Solid symbols are measured values and open diamonds are calculated from the data shown in Fig. 6.

The effective particle density (ρ_{eff}) values were calculated by comparing vacuum aerodynamic diameter (D_{va}) values from AMS measurements in PTOF mode with SMPS mobility diameters with the following equation assuming that the particles are spherical and contain no internal voids: (DeCarlo et al., 2004)

$$\rho_{\text{eff}} = D_{\text{va}}/D_m \quad (2)$$

Using Eq. (2), effective densities for the laboratory SOA are reported in Table 1. This value is consistent with particle density values for chamber SOA for similar SOA mass loadings (Bahreini et al., 2005; Shilling et al., 2009). Particle density changes with OH exposure are shown in Fig. 7. Particle density values increased linearly with OH exposures up to a maximum of approximately 10%. The increase in particle density due to heterogeneous oxidation, consistent with increased particle oxidation, has also been observed in our previous work with model POA particles with up to approximately 20% increase in particle densities (George et al., 2007; Kroll et al., 2009).

Volume and density changes were used to calculate expected mass changes, which were compared with observed changes in AMS organic mass normalized to particle number concentrations, as shown in Fig. 8. Variability in normalized organic mass was within 17% under control conditions. Although there were a few data points showing a net increase in organic mass, most data showed a trend of loss of organic mass with OH exposure. Due to the high variability, most of these data were not statistically different from control data. Calculated mass changes showed no significant mass loss consistent with measured values, except for high OH exposures $\geq 8\times10^{-8}$ atm-s. At these high exposures measured mass changes were significantly different from calculated values. In comparison, a mass reduction of approximately 7% would be expected for oxidized squalane particles for a comparable starting O/C ratio as the SOA particles and over 3 OH lifetimes (Kroll et al., 2009).

The modification of the CCN activity of SOA1 and SOA2 particles due to heterogeneous oxidation was determined by measuring the activation diameter (D_{act}) for an effective chamber supersaturation of S_{eff} =0.32%. Given the similarity in SOA types, SOA3 was not studied. Figure 9 shows average hygroscopicity parameter (κ) values (Petters and Kreidenweis, 2007) under different flow tube conditions averaged over both SOA types. As shown in Fig. 9a, κ values for SOA particles sampled directly, i.e. before dilution with other flows, bypassing the activated carbon denuders and the flow tube setup ("No C Traps"), did not vary significantly with the addition of activated carbon denuders ("C traps"). A comparison of average κ values of SOA under different control conditions indicates that there appears to be an increase in CCN activity under Dark O_3 and Hg Lamp conditions compared to Dark conditions with no O_3 present. Nevertheless, the differences between values under control conditions are not statistically significant. The κ values under all control conditions ranged from κ=0.08–0.16. The observed κ values are consistent with literature κ values derived from CCN measurements of chamber α-pinene SOA (Hartz et al., 2005; Prenni et al., 2007; Duplissy et al., 2008; Engelhart et al., 2008; Wex et al., 2009).

Note that we have made the assumption in these experiments that the hygroscopicities of SOA particles are initially constant with particle size. We observed relatively broad CCN activation curves however, suggesting that there is some variability in hygroscopicities with particle size that may have contributed to variability in our results. Although the mass spectra for SOA particles did not change

significantly under the Hg Lamp and O_3 Dark control conditions, it is possible that particle composition could still have been altered on a molecular level that may impact the CCN activity, as the extent of the changes may vary with particle size. This may explain why the variability in the CCN activation results appears to increase when SOA particles are exposed to UV light (Hg Lamp), O_3 Dark as well as OH, but more work is needed to confirm this. Furthermore, because oxidation rates may vary with particle size, there may also be chemical variability from size to size in the oxidized polydisperse aerosol. Another possibility is that not all particles receive the same level of OH exposure in the flow reactor.

The average κ value for both SOA1 and SOA2 particles is also included in Fig. 9. SOA particles were reacted during each CCN experiment with an average OH exposure of 5.1×10^{-8} atm-s, an equivalent atmospheric OH exposure of two weeks. In general, we observed an increase in CCN activity when SOA particles were exposed to OH radicals with an average κ value of κ=0.17±0.03, but the increases in hygroscopicity were not significant when considering the variability in the averaged data for both SOA types. The variability in the activation diameters and κ values for both averaged control and OH data were more pronounced in the SOA2 than the SOA1, as shown in Fig. 9b. Kappa values for both SOA1 (κ=0.098 (±0.005)) and SOA2 (κ=0.12(±0.03)) were in general agreement. When discriminating between SOA types, the enhanced CCN activity of SOA1 due to OH reaction compared to control conditions was statistically significant, whereas changes for SOA2 were not. The κ values for SOA1 increased by 74% to an average value of κ=0.17(±0.02).

Overall, the changes in hygroscopicity observed for SOA particles were less dramatic than what has been previously observed for model POA during OH oxidation, where κ values were observed to increase from ∼0 up to 0.08 (George et al., 2009). Because POA is initially hydrophobic (κ ∼0), its hygroscopicity is much more sensitive to the addition of small amounts of soluble material and surface tension reduction than SOA particles of relatively moderate hygroscopicity. One possible reason for these differences is the role of surface tension, which may be important for oxidized POA containing surface active species compared to SOA particles containing more highly soluble organics that may not be as surface active. SOA chamber studies have indicated that photochemical aging over several hours (<24 h) has a small effect on CCN activity of α-pinene SOA particles (Duplissey et al., 2008; Juranyi et al., 2009) with a maximum observed change in the CCN-derived hygroscopicity factor of 0.03. Yet, κ values derived from hygroscopic growth measurements at subsaturated relative humidities was more significantly enhanced from aging compared to the CCN measurements. One possible explanation is that surface active species will have a greater impact on surface tension under subsaturated conditions, where their concentrations in the particle are higher (Juranyi et al., 2009). It is possible that heterogeneous oxidation may impact hygroscopic growth of organic aerosols over the timescale of days as has been shown for photochemical aging of chamber SOA over shorter timescales, but such measurements have not yet been conducted.

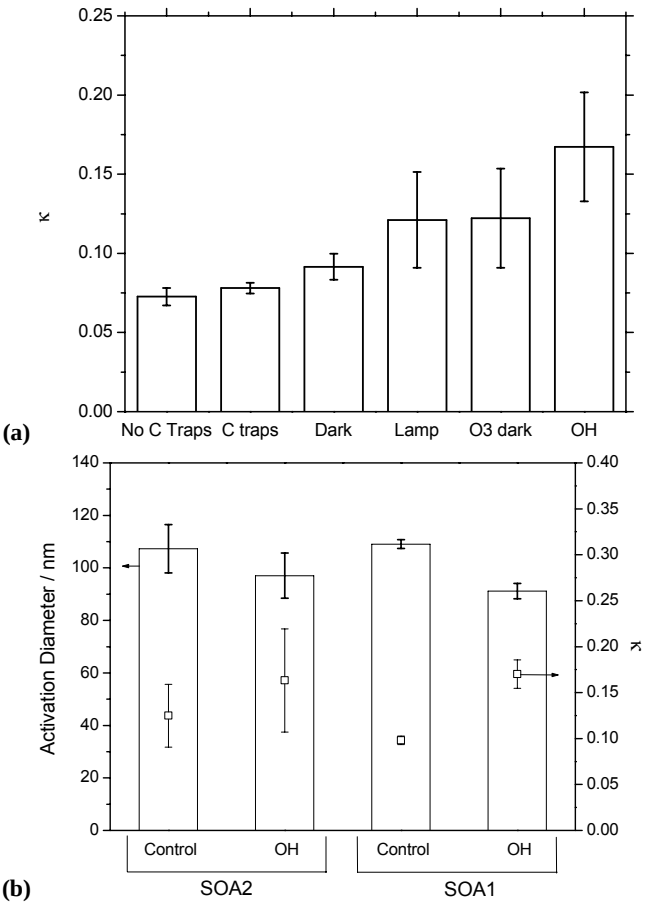

Fig. 9. (a) Average κ values for various flow tube control conditions and for an average OH exposure of 5.1×10^{-8} atm-s for the "OH" column. **(b)** Activation diameter (bars) and corresponding κ values (squares) of SOA2 and SOA1 for control conditions and for OH exposure conditions. CCN experiments were conducted under an effective supersaturation of S_{eff}=0.32%. Error bars represent one standard deviation of mean values.

4 Atmospheric implications and conclusions

We sought to determine whether heterogeneous oxidation could enhance the degree of oxidation of SOA particles under atmospherically relevant timescales, and to assess the concomitant changes in aerosol properties. This work, in combination with our related work on OH oxidation of ambient aerosols (George et al., 2008; George, 2009), demonstrates that relatively oxygenated organic aerosol particles reach an enhanced degree of oxidation from heterogeneous

oxidation under atmospherically relevant timescales, with the O/C ratios estimated from F44 values increasing from O/C=0.25–0.35 initially (i.e. F44=0.04–0.07) by approximately ΔO/C$\sim$0.04 (i.e. ΔF44$\sim$0.01) at the atmospherically relevant OH exposures of 2 weeks assuming a 24-h average OH concentration of 10^6 cm^{-3}. A comparison of these aging studies along with our work on model POA (George et al., 2007) leads to the generalized conclusion that POA-like particles undergo more dramatic chemical transformations than SOA on a relative scale due to OH oxidation. This is due to the fact that POA particles have low initial oxygen content (O/C$<$0.1), minor changes from oxidation will obviously have a greater impact on their overall composition than for SOA particles. The changes in degree of oxidation from OH oxidative processing are consistent for POA and SOA with an enhancement in O/C ratio of up to ΔO/C$\sim$0.08 for two weeks of heterogeneous reaction with OH.

The PMF factors that were deconvolved from the SOA organic mass spectra were similar to ambient OOA and HOA PMF factors. For one day of atmospheric OH aging, our work suggests that observed changes are not likely to impact organic aerosol composition compared to chemical aging expected from an increase in OOA due to SOA formation that occurs on a timescale of several hours in areas with high VOC mixing ratios, such as urban regions. However, our results indicate that OH oxidation over two weeks reduced the HOA-like fraction and increased the OOA fraction by approximately 11% of total organic mass (i.e. the OOA fraction increased from 0.34 to $\sim$0.45) of the laboratory SOA particles. In this respect, we are in general agreement with the aging experiments reported in Jimenez et al. (2009). But we do note that an OH exposure of two weeks did not fully transform SOA to the composition of highly oxygenated, aged OOA (i.e. OOA1 or LV-OOA). In particular, the O/C ratio did not increase past O/C=0.45 under the OH exposures in this work, whereas ambient OOA1/LV-OOA has been observed to have O/C ratios in the range of approximately O/C=0.5–0.9 (Ng et al., 2009). Although difficult to extrapolate from just one lab study, these results suggest that heterogeneous OH oxidation is not the dominant aging mechanism for the conversion of OA to the most highly oxidized form of OOA. Additional aging mechanisms, such as SOA formation, oxidative aging of semi-volatiles organics, cloud processing, and coagulation with particles containing soluble organics, likely also play an important role in the transformation of atmospheric organic aerosol to low-volatility OOA1. Heterogeneous oxidation could be a significant aging process leading to OOA formation from POA and SOA in remote regions with lower VOC mixing ratios compared to urban regions.

The observed changes in particle composition were accompanied by modifications in physical properties of SOA particles. As observed in our previous work, with the exception of solid model POA particles (George et al., 2007, 2008; Hearn et al., 2007; Kroll et al., 2009), a minor fraction of monodisperse SOA particle volume was volatilized, i.e. up to 10% for SOA and 20% for POA particles, from OH oxidation under atmospherically relevant exposures. SOA particle densities were enhanced due to aging as a result of an increase in particle-phase oxygenated species. The freshly generated SOA particles readily acted as CCN under atmospheric supersaturations, and thus the modification in SOA hygroscopicity from OH oxidation was less significant compared to hygroscopicity changes observed in previous work with model POA (Petters et al., 2006; George et al., 2009). These differences are likely because the SOA components may not be as surface active as oxidized hydrophobic compounds (Asa-Awuku et al., 2008). Another possibility for the less dramatic modification in particle properties of SOA during oxidation compared to model POA on the whole is slower kinetics of oxidation. It is currently unclear whether OH uptake remains constant as OA particles become more oxidized. Although OH oxidation may not significantly alter CCN activity of OOA, it may nevertheless lead to an enhancement of the particle hygroscopic growth if surface active species are produced, but more work is needed to explore this possibility. Close to source regions, it is now becoming clear that other particle aging pathways, such as condensation of inorganic material and SOA, will likely dominate the conversion of POA to more hydrophilic and CCN active OA.

Supplementary material related to this article is available online at:
http://www.atmos-chem-phys.net/10/5551/2010/acp-10-5551-2010-supplement.acp-2010-56-supplement.pdf.

Acknowledgements. Funding for this work was provided by NSERC and infrastructure funding was provided by CFI/OIT.

Edited by: J. N. Crowley

References

Aiken, A. C., Decarlo, P. F., Kroll, J. H., Worsnop, D. R., Huffman, J. A., Docherty, K. S., Ulbrich, I. M., Mohr, C., Kimmel, J. R., Sueper, D., Sun, Y., Zhang, Q., Trimborn, A., Northway, M., Ziemann, P. J., Canagaratna, M. R., Onasch, T. B., Alfarra, M. R., Prevot, A. S. H., Dommen, J., Duplissy, J., Metzger, A., Baltensperger, U., and Jimenez, J. L.: O/C and OM/OC ratios of primary, secondary, and ambient organic aerosols with high-resolution time-of-flight aerosol mass spectrometry, Environ. Sci. Technol., 42, 4478–4485, 2008.

Alfarra, M. R., Paulsen, D., Gysel, M., Garforth, A. A., Dommen, J., Prèvôt, A. S. H., Worsnop, D. R., Baltensperger, U., and Coe, H.: A mass spectrometric study of secondary organic aerosols formed from the photooxidation of anthropogenic and biogenic precursors in a reaction chamber, Atmos. Chem. Phys., 6, 5279–5293, doi:10.5194/acp-6-5279-2006, 2006.

Asa-Awuku, A., Sullivan, A. P., Hennigan, C. J., Weber, R. J., and Nenes, A.: Investigation of molar volume and surfactant characteristics of water-soluble organic compounds in biomass burning

aerosol, Atmos. Chem. Phys., 8, 799–812, doi:10.5194/acp-8-799-2008, 2008.

Bahreini, R., Keywood, M. D., Ng, N. L., Varutbangkul, V., Gao, S., Flagan, R. C., Seinfeld, J. H., Worsnop, D. R., and Jimenez, J. L.: Measurements of secondary organic aerosol from oxidation of cycloalkenes, terpenes, and m-xylene using an Aerodyne aerosol mass spectrometer, Environ. Sci. Technol., 39, 5674–5688, 2005.

Baltensperger, U., Kalberer, M., Dommen, J., Paulsen, D., Alfarra, M. R., Coe, H., Fisseha, R., Gascho, A., Gysel, M., Nyeki, S., Sax, M., Steinbacher, M., Prevot, A. S. H., Sjogren, S., Weingartner, E., and Zenobi, R.: Secondary organic aerosols from anthropogenic and biogenic precursors, Faraday Discuss., 130, 265–278, 2005.

Bertram, A. K., Ivanov, A. V., Hunter, M., Molina, L. T., and Molina, M. J.: The reaction probability of OH on organic surfaces of tropospheric interest, J. Phys. Chem. A, 105, 9415–9421, 2001.

Broekhuizen, K. E., Thornberry, T., Kumar, P. P., and Abbatt, J. P. D.: Formation of cloud condensation nuclei by oxidative processing: Unsaturated fatty acids, J. Geophys. Res. Atmos., 109, D24206, doi:10.1029/2004JD005298, 2004.

de Gouw, J. A., Middlebrook, A. M., Warneke, C., Goldan, P. D., Kuster, W. C., Roberts, J. M., Fehsenfeld, F. C., Worsnop, D. R., Canagaratna, M. R., Pszenny, A. A. P., Keene, W. C., Marchewka, M., Bertman, S. B., and Bates, T. S.: Budget of organic carbon in a polluted atmosphere: Results from the New England Air Quality Study in 2002, J. Geophys. Res. Atmos., 110, D16305, doi:10.1029/2004JD005623, 2005.

DeCarlo, P. F., Slowik, J. G., Worsnop, D. R., Davidovits, P., and Jimenez, J. L.: Particle morphology and density characterization by combined mobility and aerodynamic diameter measurements. Part 1: Theory, Aerosol Sci. Technol., 38, 1185–1205, 2004.

Drewnick, F., Hings, S. S., DeCarlo, P., Jayne, J. T., Gonin, M., Fuhrer, K., Weimer, S., Jimenez, J. L., Demerjian, K. L., Borrmann, S., and Worsnop, D. R.: A new time-of-flight aerosol mass spectrometer (TOF-AMS) – Instrument description and first field deployment, Aerosol Sci. Technol., 39, 637–658, 2005.

Duplissy, J., Gysel, M., Alfarra, M. R., Dommen, J., Metzger, A., Prevot, A. S. H., Weingartner, E., Laaksonen, A., Raatikainen, T., Good, N., Turner, S. F., McFiggans, G., and Baltensperger, U.: Cloud forming potential of secondary organic aerosol under near atmospheric conditions, Geophys. Res. Lett., 35, L03818, doi:10.1029/2007GL031075, 2008.

Eliason, T. L., Gilman, J. B., and Vaida, V.: Oxidation of organic films relevant to atmospheric aerosols, Atmos. Environ., 38, 1367–1378, 2004.

Engelhart, G. J., Asa-Awuku, A., Nenes, A., and Pandis, S. N.: CCN activity and droplet growth kinetics of fresh and aged monoterpene secondary organic aerosol, Atmos. Chem. Phys., 8, 3937–3949, doi:10.5194/acp-8-3937-2008, 2008.

George, I. J., Vlasenko, A., Slowik, J. G., Broekhuizen, K., and Abbatt, J. P. D.: Heterogeneous oxidation of saturated organic aerosols by hydroxyl radicals: uptake kinetics, condensed-phase products, and particle size change, Atmos. Chem. Phys., 7, 4187–4201, doi:10.5194/acp-7-4187-2007, 2007.

George, I. J., Slowik, J., and Abbatt, J. P. D.: Chemical aging of ambient organic aerosol from heterogeneous reaction with hydroxyl radicals, Geophys. Res. Lett., 35, L13811, doi:10.1029/2008GL033884, 2008.

George, I. J.: OH-initiated heterogeneous oxidation of atmospheric organic aerosols, Ph.D. Dissertation thesis, University of Toronto, Toronto, 2009.

George, I. J., Chang, R. Y.-W., Danov, V., Vlasenko, A., and Abbatt, J. P. D.: Modification of Cloud Condensation Nucleus Activity of Organic Aerosols by Hydroxyl Radical Heterogeneous Oxidation, Atmos. Environ., 43, 5038–5045, 2009.

Goldstein, A. H. and Galbally, I. E.: Known and unexplored organic constituents in the earth's atmosphere, Environ. Sci. Technol., 41, 1514–1521, 2007.

Gross, S. and Bertram, A. K.: Products and kinetics of the reactions of an alkane monolayer and a terminal alkene monolayer with NO_3 radicals, J. Geophys. Res., 114, D02307, doi:10.1029/2008JD010987, 2009.

Gross, S., Iannone, S. X., Xiao, S., and Bertram, A. K.: Reactive uptake studies of NO_3 and N_2O_5 on alkenoic acid, alkanoate, and polyalcohol substrates to probe nighttime aerosol chemistry, Phys. Chem. Chem. Phys., 11, 7792–7803, 2009.

Hartz, K. E. H., Rosenorn, T., Ferchak, S. R., Raymond, T. M., Bilde, M., Donahue, N. M., and Pandis, S. N.: Cloud condensation nuclei activation of monoterpene and sesquiterpene secondary organic aerosol, J. Geophys. Res., 110, D14208, doi:10.1029/2004JD005754, 2005.

Heald, C. L., Goldstein, A. H., Allan, J. D., Aiken, A. C., Apel, E., Atlas, E. L., Baker, A. K., Bates, T. S., Beyersdorf, A. J., Blake, D. R., Campos, T., Coe, H., Crounse, J. D., DeCarlo, P. F., de Gouw, J. A., Dunlea, E. J., Flocke, F. M., Fried, A., Goldan, P., Griffin, R. J., Herndon, S. C., Holloway, J. S., Holzinger, R., Jimenez, J. L., Junkermann, W., Kuster, W. C., Lewis, A. C., Meinardi, S., Millet, D. B., Onasch, T., Polidori, A., Quinn, P. K., Riemer, D. D., Roberts, J. M., Salcedo, D., Sive, B., Swanson, A. L., Talbot, R., Warneke, C., Weber, R. J., Weibring, P., Wennberg, P. O., Worsnop, D. R., Wittig, A. E., Zhang, R., Zheng, J., and Zheng, W.: Total observed organic carbon (TOOC) in the atmosphere: a synthesis of North American observations, Atmos. Chem. Phys., 8, 2007–2025, doi:10.5194/acp-8-2007-2008, 2008.

Hearn, J. D., Renbaum, L. H., Wang, X., and Smith, G. D.: Kinetics and products from reaction of Cl radicals with dioctyl sebacate (DOS) particles in O_2: a model for radical-initiated oxidation of organic aerosols, Phys. Chem. Chem. Phys., 9, 4803–4813, 2007.

Jayne, J. T., Leard, D. C., Zhang, X. F., Davidovits, P., Smith, K. A., Kolb, C. E., and Worsnop, D. R.: Development of an aerosol mass spectrometer for size and composition analysis of submicron particles, Aerosol Sci. Tech., 33, 49–70, 2000.

Jimenez, J. L., Canagaratna, M. R., Donahue, N. M., Prevot, A. S. H., Zhang, Q., Kroll, J. H., DeCarlo, P. F., Allan, J. D., Coe, H., Ng, N. L., Aiken, A. C., Docherty, K. S., Ulbrich, I. M., Grieshop, A. P., Robinson, A. L., Duplissy, J., Smith, J. D., Wilson, K. R., Lanz, V. A., Hueglin, C., Sun, Y. L., Tian, J., Laaksonen, A., Raatikainen, T., Rautiainen, J., Vaattovaara, P., Ehn, M., Kulmala, M., Tomlinson, J. M., Collins, D. R., Cubison, M. J., E., Dunlea, J., Huffman, J. A., Onasch, T. B., Alfarra, M. R., Williams, P. I., Bower, K., Kondo, Y., Schneider, J., Drewnick, F., Borrmann, S., Weimer, S., Demerjian, K., Salcedo, D., Cottrell, L., Griffin, R., Takami, A., Miyoshi, T., Hatakeyama, S., Shimono, A., Sun, J. Y., Zhang, Y. M., Dzepina, K., Kimmel, J. R., Sueper, D., Jayne, J. T., Herndon, S. C., Trimborn, A. M., Williams, L. R., Wood, E. C., Middlebrook, A. M., Kolb, C. E.,

Baltensperger, U., and Worsnop, D. R.: Evolution of Organic Aerosols in the Atmosphere, Science, 326, 1525–1529, 2009.

Juranyi, Z., Gysel, M., Duplissy, J., Weingartner, E., Tritscher, T., Dommen, J., Henning, S., Ziese, M., Kiselev, A., Stratmann, F., George, I., and Baltensperger, U.: Influence of gas-to-particle partitioning on the hygroscopic and droplet activation behaviour of α-pinene secondary organic aerosol, Phys. Chem. Chem. Phys., 11, 8091–8097, 2009.

Kanakidou, M., Seinfeld, J. H., Pandis, S. N., Barnes, I., Dentener, F. J., Facchini, M. C., Van Dingenen, R., Ervens, B., Nenes, A., Nielsen, C. J., Swietlicki, E., Putaud, J. P., Balkanski, Y., Fuzzi, S., Horth, J., Moortgat, G. K., Winterhalter, R., Myhre, C. E. L., Tsigaridis, K., Vignati, E., Stephanou, E. G., and Wilson, J.: Organic aerosol and global climate modelling: a review, Atmos. Chem. Phys., 5, 1053–1123, doi:10.5194/acp-5-1053-2005, 2005.

Kleinman, L. I., Daum, P. H., Lee, Y. N., Senum, G. I., Springston, S. R., Wang, J., Berkowitz, C., Hubbe, J., Zaveri, R. A., Brechtel, F. J., Jayne, J., Onasch, T. B., and Worsnop, D.: Aircraft observations of aerosol composition and ageing in New England and Mid-Atlantic States during the summer 2002 New England Air Quality Study field campaign, J. Geophys. Res. Atmos., 112, D09310, doi:10.1029/2006JD0077862007.

Knopf, D. A., Mak, J., Gross, S., and Bertram, A. K.: Does atmospheric processing of saturated hydrocarbon surfaces by NO_3 lead to volatilization?, Geophys. Res. Lett., 33, L17816, doi:10.1029/2006GL026884, 2006.

Kroll, J. H., Smith, J. D., Che, D. L., Kessler, S. H., Worsnop, D. R., and Wilson, K. R.: Measurement of fragmentation and functionalization pathways in the heterogeneous oxidation of oxidized organic aerosol, Phys. Chem. Chem. Phys., 11, 8005–8014, 2009.

Pradeep Kumar, P., Broekhuizen, K., and Abbatt, J. P. D.: Organic acids as cloud condensation nuclei: Laboratory studies of highly soluble and insoluble species, Atmos. Chem. Phys., 3, 509–520, doi:10.5194/acp-3-509-2003, 2003.

Lambe, A. T., Zhang, J. Y., Sage, A. M., and Donahue, N. M.: Controlled OH radical production via ozone-alkene reactions for use in aerosol aging studies, Environ. Sci. Technol., 41, 2357–2363, 2007.

Lanz, V. A., Alfarra, M. R., Baltensperger, U., Buchmann, B., Hueglin, C., and Prèvôt, A. S. H.: Source apportionment of submicron organic aerosols at an urban site by factor analytical modelling of aerosol mass spectra, Atmos. Chem. Phys., 7, 1503–1522, doi:10.5194/acp-7-1503-2007, 2007.

McFiggans, G., Alfarra, M. R., Allan, J., Bower, K., Coe, H., Cubison, M., Topping, D., Williams, P., Decesari, S., Facchini, C., and Fuzzi, S.: Simplification of the representation of the organic component of atmospheric particulates, Faraday Discuss., 130, 341–362, 2005.

McNeill, V. F., Yatavelli, R. L. N., Thornton, J. A., Stipe, C. B., and Landgrebe, O.: Heterogeneous OH oxidation of palmitic acid in single component and internally mixed aerosol particles: vaporization and the role of particle phase, Atmos. Chem. Phys., 8, 5465–5476, doi:10.5194/acp-8-5465-2008, 2008.

Moise, T. and Rudich, Y.: Uptake of Cl and Br by organic surfaces – a perspective on organic aerosols processing by tropospheric oxidants, Geophys. Res. Lett., 28, 4083–4086, 2001.

Molina, M. J., Ivanov, A. V., Trakhtenberg, S., and Molina, L. T.: Atmospheric evolution of organic aerosol, Geophys. Res. Lett., 31, L22104, doi:10.1029/2004GL020910, 2004.

Ng, N. L., Canagaratna, M. R., Zhang, Q., Jimenez, J. L., Tian, J., Ulbrich, I. M., Kroll, J. H., Docherty, K. S., Chhabra, P. S., Bahreini, R., Murphy, S. M., Seinfeld, J. H., Hildebrandt, L., Donahue, N. M., DeCarlo, P. F., Lanz, V. A., Prévôt, A. S. H., Dinar, E., Rudich, Y., and Worsnop, D. R.: Organic aerosol components observed in Northern Hemispheric datasets from Aerosol Mass Spectrometry, Atmos. Chem. Phys., 10, 4625–4641, doi:10.5194/acp-10-4625-2010, 2010.

Paatero, P. and Tapper, U.: Positive Matrix Factorization – a Nonnegative Factor Model with Optimal Utilization of Error-Estimates of Data Values, Environmetrics, 5, 111–126, 1994.

Paatero, P.: Least squares formulation of robust non-negative factor analysis, Chemom. Intell. Lab. Syst., 37, 23–35, 1997.

Petters, M. D., Prenni, A. J., Kreidenweis, S. M., DeMott, P. J., Matsunaga, A., Lim, Y. B., and Ziemann, P. J.: Chemical aging and the hydrophobic-to-hydrophilic conversion of carbonaceous aerosol, Geophys. Res. Lett., 33, L24806, doi:10.1029/2006GL027249, 2006.

Petters, M. D. and Kreidenweis, S. M.: A single parameter representation of hygroscopic growth and cloud condensation nucleus activity, Atmos. Chem. Phys., 7, 1961–1971, doi:10.5194/acp-7-1961-2007, 2007.

Prenni, A. J., Petters, M. D., Kreidenweis, S. M., DeMott, P. J., and Ziemann, P. J.: Cloud droplet activation of secondary organic aerosol, J Geophys Res. Atmos., 112, D10223, doi:10.1029/2006JD007963, 2007.

Renbaum, L. H. and Smith, G. D.: The importance of phase in the radical-initiated oxidation of model organic aerosols: reactions of solid and liquid brassidic acid particles, Phys. Chem. Chem. Phys., 11, 2441–2451, 2009.

Robinson, A. L., Donahue, N. M., Shrivastava, M. K., Weitkamp, E. A., Sage, A. M., Grieshop, A. P., Lane, T. E., Pierce, J. R., and Pandis, S. N.: Rethinking organic aerosols: Semivolatile emissions and photochemical aging, Science, 315, 1259–1262, 2007.

Rudich, Y., Donahue, N. M., and Mentel, T. F.: Aging of organic aerosol: Bridging the gap between laboratory and field studies, Annu. Rev. Phys. Chem., 58, 321–352, 2007.

Sage, A. M., Weitkamp, E. A., Robinson, A. L., and Donahue, N. M.: Evolving mass spectra of the oxidized component of organic aerosol: results from aerosol mass spectrometer analyses of aged diesel emissions, Atmos. Chem. Phys., 8, 1139–1152, doi:10.5194/acp-8-1139-2008, 2008.

Shilling, J. E., King, S. M., Mochida, M., and Martin, S. T.: Mass spectral evidence that small changes in composition caused by oxidative aging processes alter aerosol CCN properties, J. Phys. Chem. A, 111, 3358–3368, 2007.

Shilling, J. E., Chen, Q., King, S. M., Rosenoern, T., Kroll, J. H., Worsnop, D. R., DeCarlo, P. F., Aiken, A. C., Sueper, D., Jimenez, J. L., and Martin, S. T.: Loading-dependent elemental composition of α-pinene SOA particles, Atmos. Chem. Phys., 9, 771–782, doi:10.5194/acp-9-771-2009, 2009.

Slowik, J. G., Stroud, C., Bottenheim, J. W., Brickell, P. C., Chang, R. Y.-W., Liggio, J., Makar, P. A., Martin, R. V., Moran, M. D., Shantz, N. C., Sjostedt, S. J., van Donkelaar, A., Vlasenko, A., Wiebe, H. A., Xia, A. G., Zhang, J., Leaitch, W. R., and Abbatt, J. P. D.: Characterization of a large biogenic secondary organic aerosol event from eastern Canadian forests, Atmos. Chem. Phys., 10, 2825–2845, doi:10.5194/acp-10-2825-2010, 2010.

Smith, J. D., Kroll, J. H., Cappa, C. D., Che, D. L., Liu, C. L., Ahmed, M., Leone, S. R., Worsnop, D. R., and Wilson, K. R.: The heterogeneous reaction of hydroxyl radicals with submicron squalane particles: a model system for understanding the oxidative aging of ambient aerosols, Atmos. Chem. Phys., 9, 3209–3222, doi:10.5194/acp-9-3209-2009, 2009.

Takegawa, N., Miyakawa, T., Kondo, Y., Blake, D. R., Kanaya, Y., Koike, M., Fukuda, M., Komazaki, Y., Miyazaki, Y., Shimono, A., and Takeuchi, T.: Evolution of submicron organic aerosol in polluted air exported from Tokyo, Geophys. Res. Lett., 33, L15814, doi:10.1029/2006GL025815, 2006.

Ulbrich, I. M., Canagaratna, M. R., Zhang, Q., Worsnop, D. R., and Jimenez, J. L.: Interpretation of organic components from Positive Matrix Factorization of aerosol mass spectrometric data, Atmos. Chem. Phys., 9, 2891–2918, doi:10.5194/acp-9-2891-2009, 2009.

Vlasenko, A., George, I. J., and Abbatt, J. P. D.: Formation of volatile organic compounds in the heterogeneous oxidation of condensed-phase organic films by gas-phase OH, J. Phys. Chem. A, 112, 1552–1560, 2008.

Weber, R. J., Sullivan, A. P., Peltier, R. E., Russell, A., Yan, B., Zheng, M., de Gouw, J., Warneke, C., Brock, C., Holloway, J. S., Atlas, E. L., and Edgerton, E.: A study of secondary organic aerosol formation in the anthropogenic-influenced southeastern United States, J. Geophys. Res. Atmos., 112, D13302, doi:10.1029/2007JD008408, 2007.

Wex, H., Petters, M. D., Carrico, C. M., Hallbauer, E., Massling, A., McMeeking, G. R., Poulain, L., Wu, Z., Kreidenweis, S. M., and Stratmann, F.: Towards closing the gap between hygroscopic growth and activation for secondary organic aerosol: Part 1 – Evidence from measurements, Atmos. Chem. Phys., 9, 3987–3997, doi:10.5194/acp-9-3987-2009, 2009.

Zahardis, J. and Petrucci, G. A.: The oleic acid-ozone heterogeneous reaction system: products, kinetics, secondary chemistry, and atmospheric implications of a model system – a review, Atmos. Chem. Phys., 7, 1237–1274, doi:10.5194/acp-7-1237-2007, 2007.

Zhang, Q., Worsnop, D. R., Canagaratna, M. R., and Jimenez, J. L.: Hydrocarbon-like and oxygenated organic aerosols in Pittsburgh: insights into sources and processes of organic aerosols, Atmos. Chem. Phys., 5, 3289–3311, doi:10.5194/acp-5-3289-2005, 2005a.

Zhang, Q., Alfarra, M. R., Worsnop, D. R., Allan, J. D., Coe, H., Canagaratna, M. R., and Jimenez, J. L.: Deconvolution and quantification of hydrocarbon-like and oxygenated organic aerosols based on aerosol mass spectrometry, Environ. Sci. Technol., 39, 4938–4952, 2005b.

Zhang, Q., Jimenez, J. L., Canagaratna, M. R., Allan, J. D., Coe, H., Ulbrich, I., Alfarra, M. R., Takami, A., Middlebrook, A. M., Sun, Y. L., Dzepina, K., Dunlea, E., Docherty, K., DeCarlo, P. F., Salcedo, D., Onasch, T., Jayne, J. T., Miyoshi, T., Shimono, A., Hatakeyama, S., Takegawa, N., Kondo, Y., Schneider, J., Drewnick, F., Borrmann, S., Weimer, S., Demerjian, K., Williams, P., Bower, K., Bahreini, R., Cottrell, L., Griffin, R. J., Rautiainen, J., Sun, J. Y., Zhang, Y. M., and Worsnop, D. R.: Ubiquity and dominance of oxygenated species in organic aerosols in anthropogenically-influenced Northern Hemisphere midlatitudes, Geophys. Res. Lett., 34, L13801, doi:10.1029/2007GL029979, 2007.